On the determination of conditional statistics along gradient trajectories at the Turbulent/Non-Turbulent Interface of jet flows.

Francisco Patiño[1*], Lea Voivenel[1], Michael Gauding[1], Luminita Danaila[1], Emilien Varea[1]

1: Normandie Univ., UNIROUEN, INSA Rouen, CNRS, CORIA, 76000 Rouen, France
*Corresponding author: patinof@coria.fr

Keywords: Conditional Statistics, PIV, PLIF, Round Jets, Gradient Trajectory.

ABSTRACT

Conditional sampling and averaging are valuable techniques for discerning and quantifying notable regions within turbulent flows. These methods have been particularly prevalent in experimental and numerical investigations of turbulent shear flows. Conditional statistics effectively analyze the dynamics and characteristics of turbulent flows, offering insights into transitional behaviors and distinct features within these regimes. This approach is instrumental in studying turbulent shear flows, such as jets or mixing layers, where a well-defined zone separates the turbulent core from the non-turbulent surrounding fluid. This zone, known as the Turbulent/Non-Turbulent Interface (TNTI), plays a crucial role in various phenomenological changes, including the transfer of mass, momentum, and scalar fluxes. While statistics in jet flows are often reported along the radial direction for a given downstream position, this method can obscure the underlying physical processes. Scalar dissipation rate, transport, or turbulent kinetic energy involve velocity or concentration gradients at the flow interface. To date, the impact of sampling direction on conditional statistics within jet flows has not yet been thoroughly discussed. This study focuses on determining gradient trajectories at the interface of turbulent flows. Gradient trajectories have been used to explore structures in turbulent flows, proving effective in analyzing homogeneous shear turbulence. This study introduces a methodology for sampling conditional data by computing gradient trajectories intersecting the TNTI. The primary objective is to verify whether sampling statistics along the gradient of scalar concentration provide a more detailed understanding of the processes occurring near the TNTI. The methodology involves computing a field of gradient trajectories from concentration fields obtained through Planar Laser-Induced Fluorescence (PLIF) in a N^2/N^2 jet with $Re = 2900$. Conditional statistics at the TNTI of a jet flow along the gradient trajectory for a given downstream position are calculated and reported. The paper aims to compare conditional statistics along gradient trajectories with those obtained along radial and normal directions at the TNTI. It is expected that gradient trajectory statistics align more closely with normal direction statistics near the interface and diverge as it gets into the jet or coflow fluid.

1. Introduction

Conditional sampling and averaging stand as valuable techniques in discerning and quantifying notable regions within turbulent flows. Their application have been notably prevalent in experimental and numerical investigations concerning turbulent shear flows. The concept of conditional statistics serves as an effective way to analyze the dynamics and characteristics of turbulent flows, offering insights into the transitional behavior and distinct features exhibited within such flow regimes. Particularly, it has found utility in studying turbulent shear flows like jets or mixing layers where a thin and well-defined zone exists and separates the turbulent core from the non-turbulent surrounding fluid. This zone is generally called the Turbulent/Non-turbulent Interface (TNTI). The TNTI plays a pivotal role in various phenomenological changes, including the transfer of mass, momentum, and scalar fluxes, as highlighted by J. Westerweel et al. (2009). Here, certain effects smoothed or hidden by the use of conventional average statistics can be highlighted. In the literature, different criteria have been applied to detect the TNTI, based on vorticity PDFs, kinetic energy, velocity, or passive scalar criteria (Da Silva et al. (2014)). Patiño et al. (2023) explored the discussion surrounding the impact of interface positioning —closely linked to the threshold technique— on conditional statistics within active or passive scalar flows. Statistics in jet flows are often reported along the radial direction for a given position downstream. However, even if this method allows for comparisons between flows, the physical underlying processes still stay hidden. Indeed, scalar dissipation rate, transport, diffusion, or dissipation involve velocity or concentration gradients that exist at the flow interface. To the author's knowledge, the impact of sampling direction on conditional statistics within the framework of jet flows has not yet been discussed. This involves the determination of gradient trajectories at the interface of turbulent flows. Gradient trajectories have been utilized to explore the central area of a shear layer, and this approach has proven effective in analyzing homogeneous shear turbulence Wang (2009b); Wang & PETERS (2008); Mellado et al. (2009). This method also enables the identification of dissipation elements, delineating regions in space where gradient trajectories reach identical minimum and maximum points. This study introduces a methodology for sampling conditional data by computing gradient trajectories intersecting the Turbulent/Non-Turbulent Interface. The primary objective is to verify whether sampling statistics along the gradient of scalar concentration provide a more detailed understanding of the processes occurring in the vicinity of the TNTI. The methodology involves computing a field of gradient trajectories derived from concentration fields obtained through Planar Laser-Induced Fluorescence (PLIF). Statistics conditioned at the TNTI of a jet flow along the gradient trajectory for a given position downstream are calculated and reported. The objectives of the paper remain twofold:

- Statistics conditioned at the TNTI of a jet flow along the gradient trajectory for a given position downstream are calculated and reported.

- A discussion is proposed on the comparison of conditional statistics along gradient trajectories and those obtained along the radial and normal directions at the TNTI.

It is expected that gradient trajectory statistics should be close to statistics along the normal direction in the vicinity of the interface and might differ further.

2. Experimental Setup

The flow facility features a round jet with a diameter D_{out} of 30 mm, surrounded by a coflow with an $800mm$ diameter (D_{cof}). This setup ensures well-defined boundary conditions. Additionally, the coflow's large diameter minimizes wall effects on the main jet and isolates it from the environment so it behaves as a free jet.

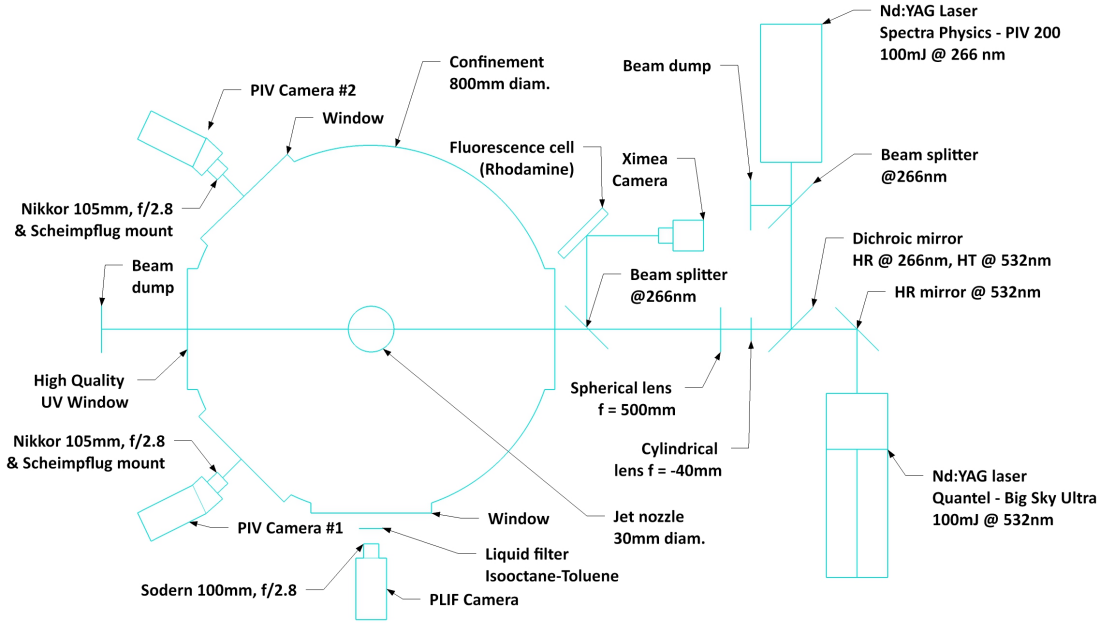

Figure 1. Sketch of the experimental device for shoot-to-shoot correction.

The main jet emerges from a contraction designed to produce a *top-hat* velocity profile at the nozzle exit, as described by Voivenel et al. (2016). To achieve this, the contraction ratio, $C_R = \frac{D_{\text{in}}^2}{D_{\text{out}}^2}$, with D_{in} as the initial diameter and D_{out} as the exit diameter, along with the length-to-initial diameter ratio $\frac{L}{D_{\text{in}}}$, were chosen based on Antonia & Zhao (2001) and Bell & Mehta (1988). The contraction ratio and the length-to-diameter ratio are $C_R = 87$ and $\frac{L}{D_{\text{in}}} \approx 1$, respectively. Velocity profiles at the nozzle exit, measured using Hot Wire Anemometry (HWA), match those reported by Antonia & Zhao (2001). The initial turbulence intensity is very low, at 1%, ensuring that measured turbulent

fluctuations are not due to injection boundary conditions. The jet's flow rate is controlled using a Coriolis Mass Flow Controller from Bronkhorst. Both dynamic and scalar fields are simultaneously measured. For this, stereoscopic PIV (Particle Image Velocimetry) and PLIF (Planar Laser Induced Fluorescence) methods are employed. For this study, measurements were made in a nitrogen jet with a nitrogen coflow. Reynolds number was set at 2900.

2.1. Dynamic Field Measurements

The stereo-PIV technique has been selected to measure the third component of the velocity (tangential direction). A Quantel Ultra Twin pulsed laser at 532 nm generates a beam that is transformed into a parallel laser sheet using a cylindrical lens ($f = -40$ mm) followed by a spherical lens ($f = 500$ mm). Figure 1 illustrates the experimental setup. The laser sheet traverses the jet center. The jet flow is seeded with Di-Ethyl-Hexyl-Sebacat (DEHS) particles, which have a more uniform size distribution than that of vegetable oil particles (approximately 1 μm in size). Two Imager ProX cameras (LaVision) equipped with Nikkor 105 mm f/2.8 lenses capture the Mie-scattering from these particles. To enhance the signal-to-noise ratio, the cameras are positioned at a 45° angle in forward scattering. Each camera records pairs of particle images, which are independently processed using Dantec's *Adaptive PIV* algorithm in *Dynamic Studio 3.4*. Through a calibration procedure, the n^{th} 2D field from camera #1 is combined with the corresponding field from camera #2, producing a single 2D-3C (two dimensions, three components) velocity field.

2.2. Concentration Measurements

While acetone molecules are typically used as tracers for Planar Laser Induced Fluorescence (PLIF) measurements, an anisole tracer is employed in this study. This molecule provides a sufficient signal-to-noise ratio even at very low seeding concentrations, as low as a few percent, as noted by Pasquier et al. (2007). Consequently, seeding does not alter the jet fluid properties. The tracer particles are excited by an Nd:YAG laser (Spectra Physics) with a fourth-harmonic generator that produces a Q-switched laser output at $\lambda = 266$ nm and 100 mJ. A dichroic mirror is used to combine the PIV laser beam with the LIF laser beam optically. The fluorescence signal is collected by an intensified CCD camera (PIMAX 4, 16 bits, 1024×1024 pixels) equipped with a UV Cerco 100 mm, $f/2.8$ lens. The exposure time is set to 500 ns, balancing between fluorescence signal collection and noise level increase. The linearity of the PLIF signal with respect to the laser energy and tracer concentration is verified. Instantaneous laser corrections for energy distribution and shot-to-shot variations are applied using a specific procedure (laser beam sampling), detailed further in Voivenel (2016). This normalization process is highly effective, significantly reducing noise compared to standard procedures.

3. TNTI Detection and Threshold Selection

The presence of a "layer" between the jet and its environment is crucial for understanding various aspects of turbulent jet flow dynamics. This layer, known as the Turbulent/Non-Turbulent Interface (TNTI), significantly influences these dynamics. According to Gampert et al. (2014), the statistics obtained from vorticity-based and passive scalar-based TNTI detection methods are similar. Therefore, we preferred to determine the interface based on the scalar field. Various thresholding methodologies can be used to identify the TNTI's position. These methods are based on a simple observation: pixels show high intensity inside the jet and low intensity outside. Thus, using a pixel intensity threshold is a logical approach. We applied this technique to corrected and normalized images to minimize errors from noise and laser sheet inhomogeneities. Consequently, the thresholding is performed on the molar fraction of the injected fluid rather than on the raw pixel intensity. To identify the interface position from the PLIF images, we followed the method proposed by T. Westerweel J.and Hofmann et al. (2002), as illustrated in Figure 2.

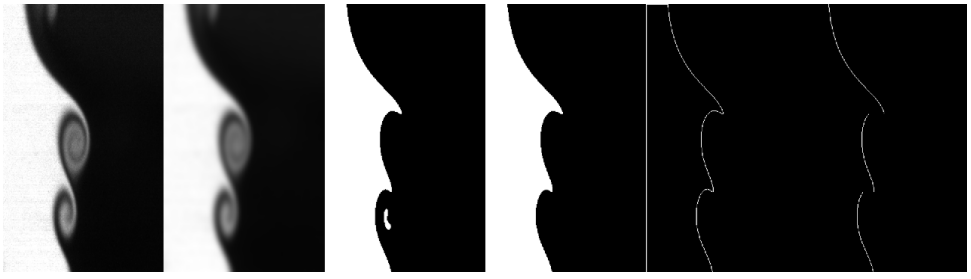

Figure 2. Step by step of obtaining the contour of the TNTI as T. Westerweel J.and Hofmann et al. (2002)

To determine the threshold value, an intuitive method is to create a histogram of the fluid concentration. The threshold value is the local minimum of the bimodal distribution, which is characteristic of the two regions. However, this bimodal distribution is not always clearly identifiable. A more universal method is presented by Prasad & Sreenivasan (1989), who propose calculating the *threshold mean intensity*. This involves calculating the average intensity over the entire threshold image for different thresholds. Two quasi-linear regions with different slopes can be identified. Pixels in the coflow have a low-intensity value, and increasing the threshold gently increases the average threshold intensity, indicating the surrounding environment. The same reasoning applies in reverse for the jet region. The threshold value is the point of intersection of these two lines. We apply the same principle to the fraction of injected fluid. This process is performed on all the instantaneous images —3000 in our case— and an average curve is calculated from the instantaneous profiles. The threshold value corresponds to the point where the second derivative cancels and changes the sign.

4. Gradient Trayectory

Gradient trajectories from 2-D experimental PLIF data are calculated over the TNTI obtained using the methodology explained before for each instantaneous scalar flow image. The processes involve the calculation of the gradient fields $\frac{\partial \phi}{\partial x}\,\frac{\partial \phi}{\partial y}$ where ϕ is the scalar quantity and x and y the streamwise and crosswise directions. Then, trajectories are calculated for each peculiar point of the image defining a segment with a typical length l. From the TNTI the starting point is given by a local maxima and the ending point by a local minima, see Wang (2009a). This method allows only one line to cross the interface at a given height.

Figure 3 shows the process of gradient line calculation that were used to get the statistics. The field of the scalar gradient can be calculated using the images from the PLIF measurements. Since the interest is to get the quantities of interest at the proximity of the interface.

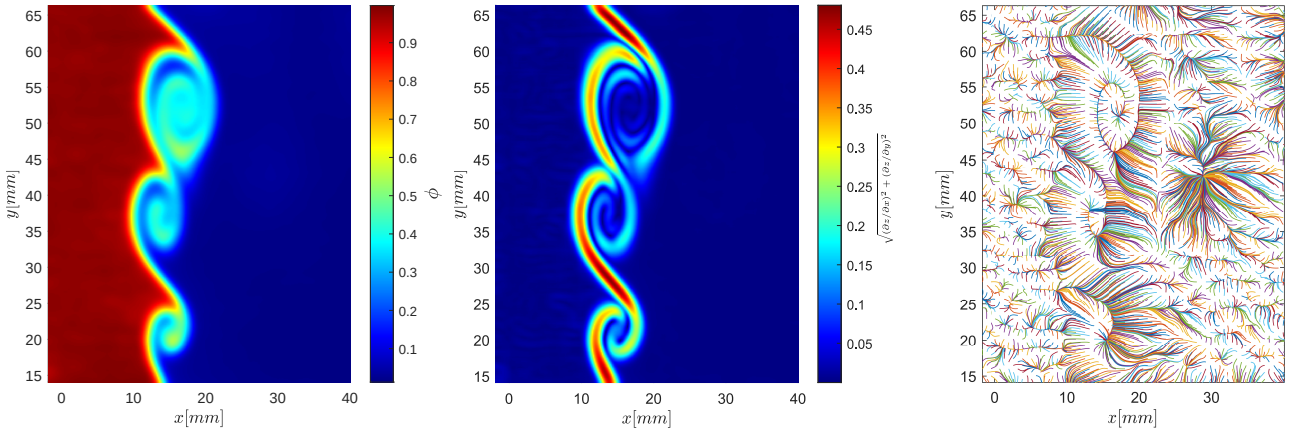

(a) (b) (c)

Figure 3. Step by step to get gradient lines to perform conditional statistics. Scalar concentration field (a). Field of the scalar gradient magnitude. (b). The complete field of gradient lines (c).

5. Results

The primary goal of this research is to assess the impact of sampling direction on conditional statistics at the interface. To achieve this, data obtained using gradient lines is compared with statistics derived from data sampled in the radial direction (perpendicular to the jet) and the direction of the normal vector to the interface.

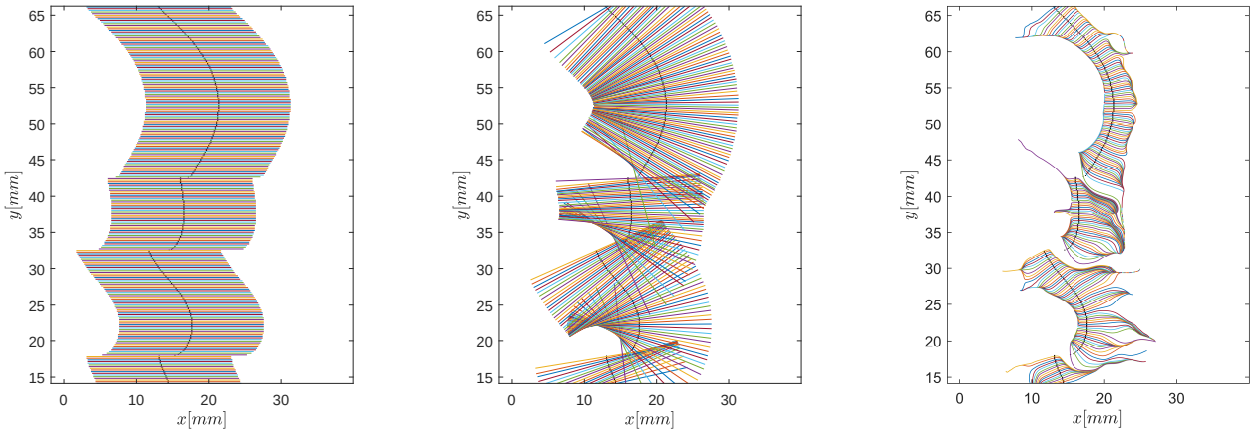

(a) Radial (b) Normal (c) Gradient

Figure 4. Difference of the sampling methods used in this research

Figure 4 illustrates the differences between the sampling points using these three methods. Sampling points in each case travel a total of 10 mm to each side from the interface or until it finds a local minima in the gradient lines case. It can be observed that the disparity among the methods becomes more pronounced at the vortices. Then, different quantities are interpolated into the lines, producing profiles for each pixel in the interface. When stacked together they create one-shot conditional maps that globally showcase the difference between the methods. Then, mean conditional fields are made by averaging all conditioned one-shots (Figure 6). Each field is the product of the processing of 3000 images. When looking at the one-shot conditional field of the scalar in Figure 5, it can be seen that the presence of Kelvin-Helmholtz instabilities is more evident in single-shot images since the normal vector from the interface points closer to the center of the vortex compared to the radial direction. It can also be noticed that there is less influence of the sampling method on the non-turbulent field when using gradient lines. Gradient lines converge in groups at local minima points on the turbulent side, sometimes completely avoiding the vortex center.

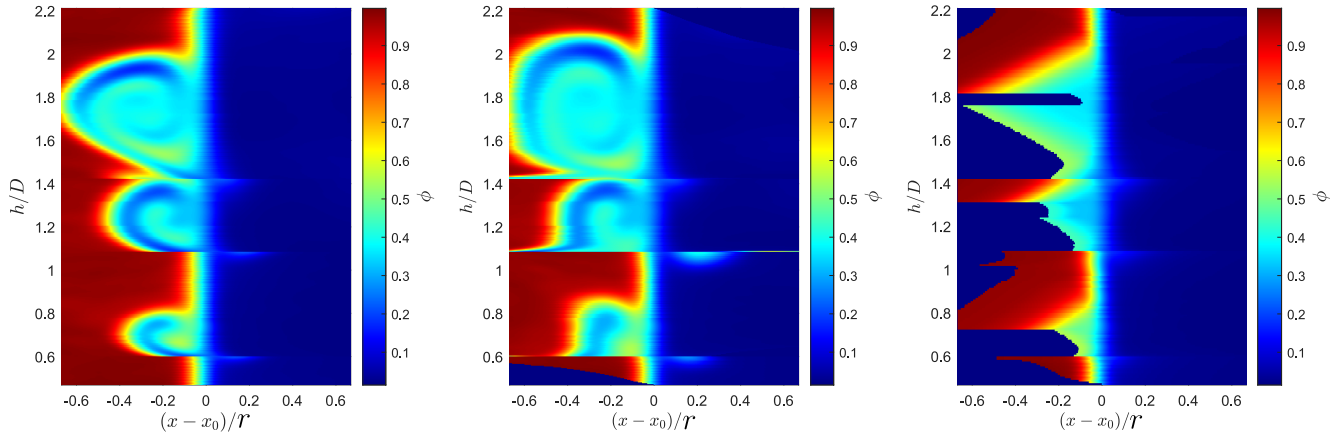

(a) Radial (b) Normal (c) Gradient

Figure 5. One-shot conditioned fields for the three methods. Height is normalized by the jet diameter and distance from the interface is normalized by the jet radius.

Then observing in Figure 5(c), it is seen that because of the direction of the gradient lines, lower and higher ends of the field are not fully filled. Indeed in the gradient line the distance sampled depends on the location of the local minima. Nevertheless, profiles at 1D and 2D are converged enough so a comparison can be done as seen in Figure 6(c).

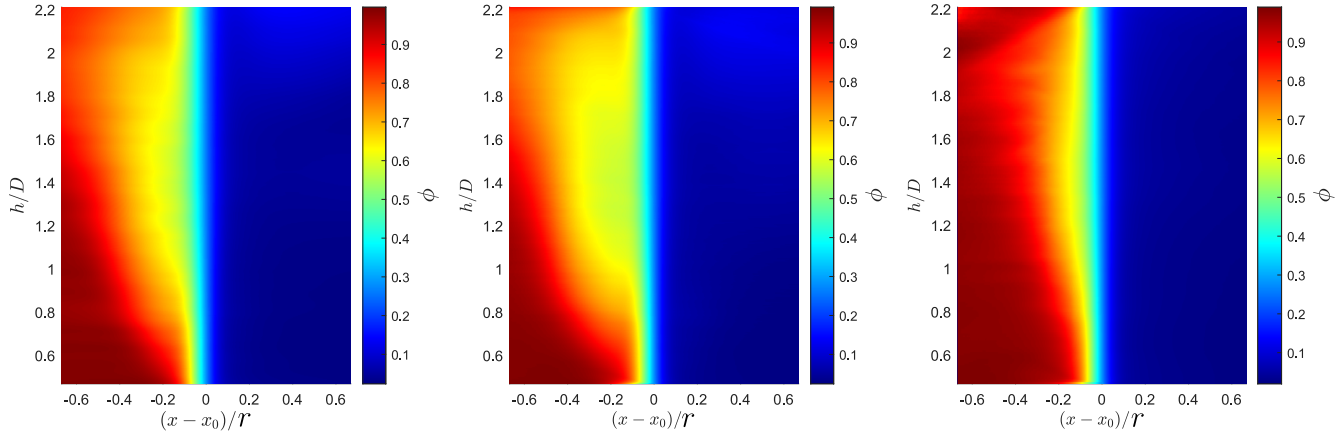

(a) Radial (b) Normal (c) Gradient

Figure 6. Mean conditioned concentration fields of the same one-shot image using different methods. Height is normalized by the jet diameter and distance from the interface is normalized by the jet radius.

The most noticeable aspect of these fields is the size of the potential core, represented by the area where the jet concentration is closer to 1. It is possible to infer that as a method takes more into

consideration the vortices, the normal case in this study, the smaller is the potential core in terms of average quantity.

5.1. Concentration Field Profiles

For the following analysis, different profiles are plotted at one and two diameters above the jet exit using the three methods. The horizontal axis represents the distance from the interface normalized by the jet radius. Therefore it is important to note that position 0 indicates the interface, negative x values correspond to the jet core, and positive x values indicate the coflow region.

Scalar concentration profiles (Figure 7) already indicates that eddies have a diminished effect on profiles when using gradient lines. While values at the interface remain unchanged, significant differences in magnitude become apparent when observed from within the jet. This observation is crucial as it refers to the region where mixing begins.

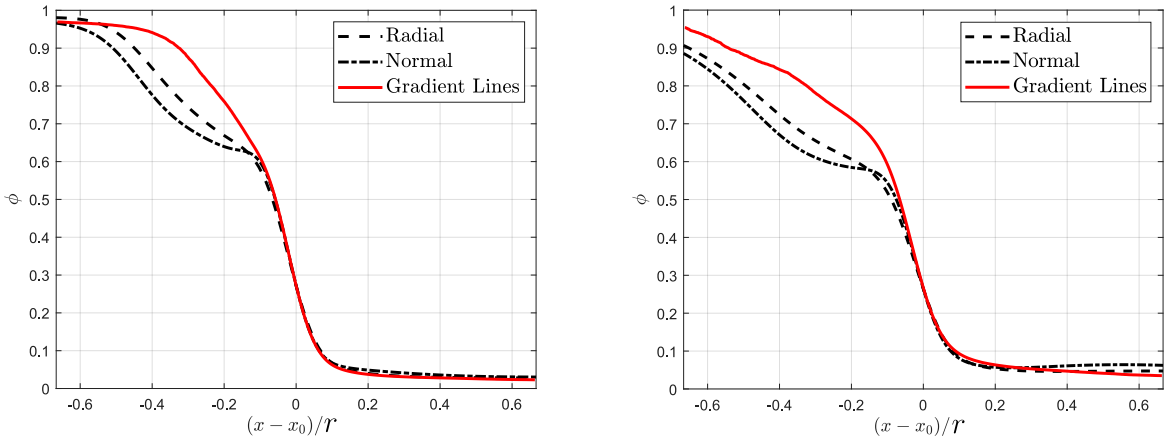

(a) 1D (b) 2D

Figure 7. Scalar concentration profiles at 1D and 2D using conditional statistics along the gradient lines compared to statistics in the radial and normal directions.

The scalar gradients, represented by the Scalar Dissipation rate in Figure 8, exhibit a smoother profile when gradient lines are utilized. This is because gradient lines are sensitive to the intrinsic flow motion, and are, to a certain extent independent of the biggest structures of the flow. Thus, Kelvin–Helmholtz structures are no longer visible. The peaks of scalar dissipation are identical across methods closer to the jet nozzle, but for gradient lines, the dissipation assumes a Gaussian distribution. It is interesting to see that when going upstream, even if the tendency regarding the shape of the curve is conserved, there is a bigger reduction of the peak for the radial and normal lines when the gradient lines remain almost unchanged.

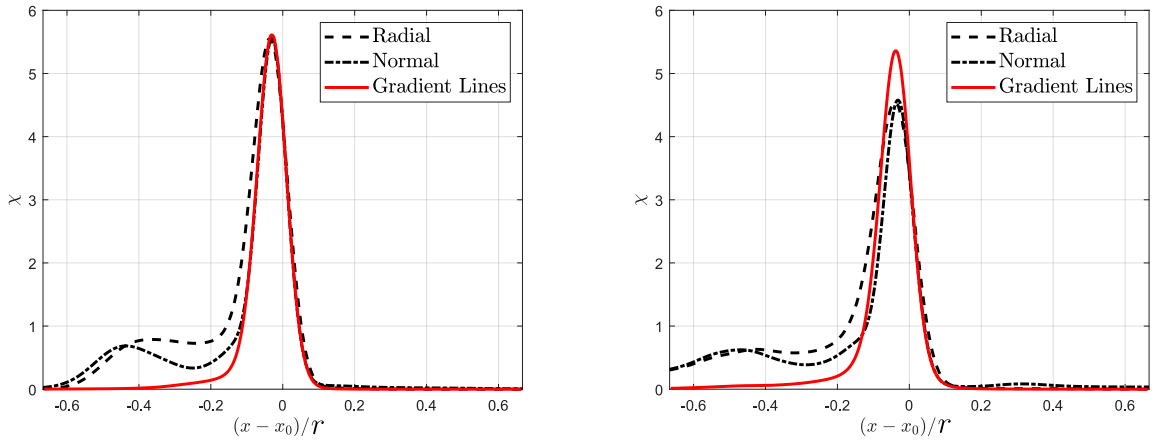

(a) 1D (b) 2D

Figure 8. Scalar dissipation rate profiles at 1D and 2D using conditional statistics along the gradient lines compared to statistics in the radial and normal direction.

5.2. Dynamic Field Profiles

In Figure 9, the magnitude of velocity at the interface is nearly identical across methods at 1D from the jet. However, in contrast to the scalar concentration, the magnitude of velocity is approximately 10% lower when using gradient lines in the jet side. But when observing at 2D, the curves significantly differ in every zone. The gradient line velocity magnitude is 60% lower in the jet zone, and 20% higher at the interface and the coflow zone.

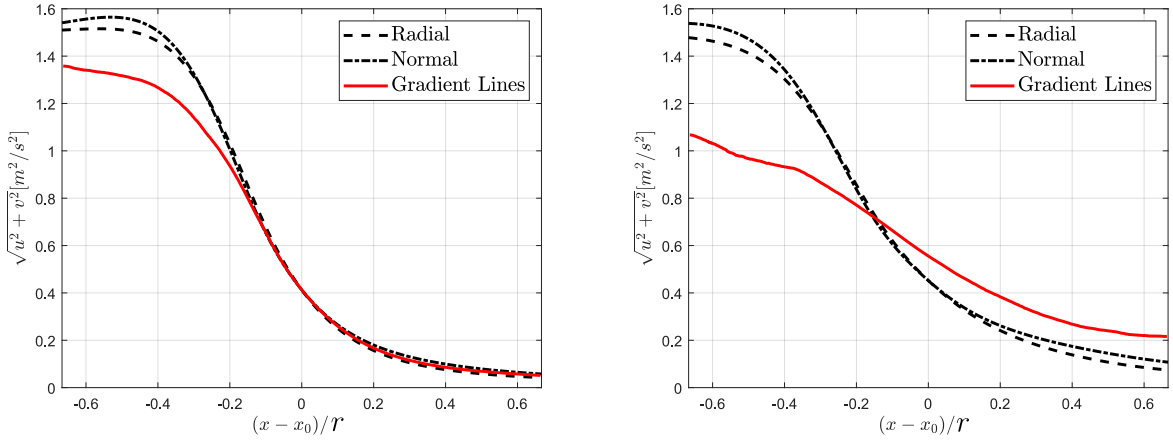

(a) 1D (b) 2D

Figure 9. Velocity magnitude profiles at 1D and 2D using conditional statistics along the gradient lines compared to statistics in the radial and normal direction.

Results for the velocity at 2D are heavily influenced by the stream-wise velocity in a whole order of magnitude as seen in Figure 10.

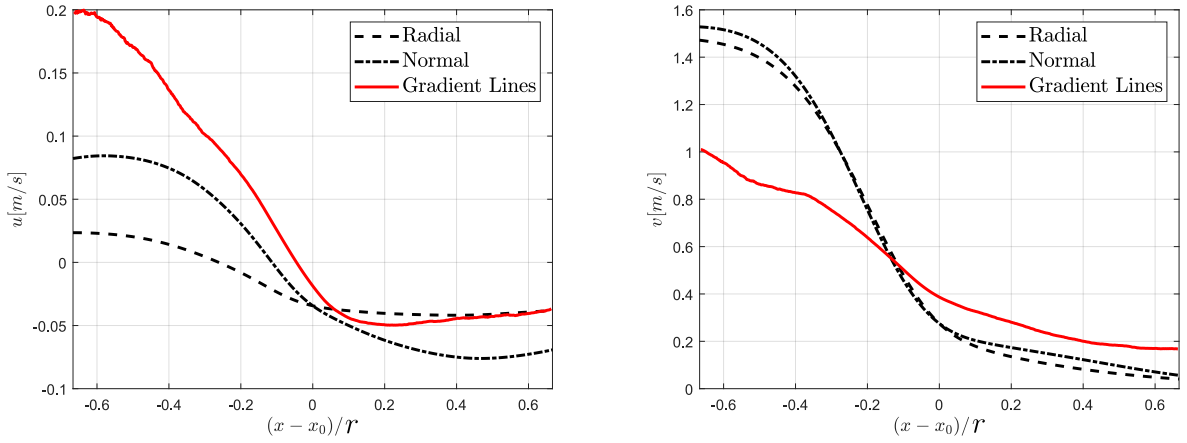

Figure 10. Velocity components at 2D. a) Axial velocity. b)Streamwise velocity.

This behaviour can be explained when looking at Figure 11. Most of the gradient lines travel through the streching part of the vortex, which have considerably lower streamwise velocity and higher radial velocity.

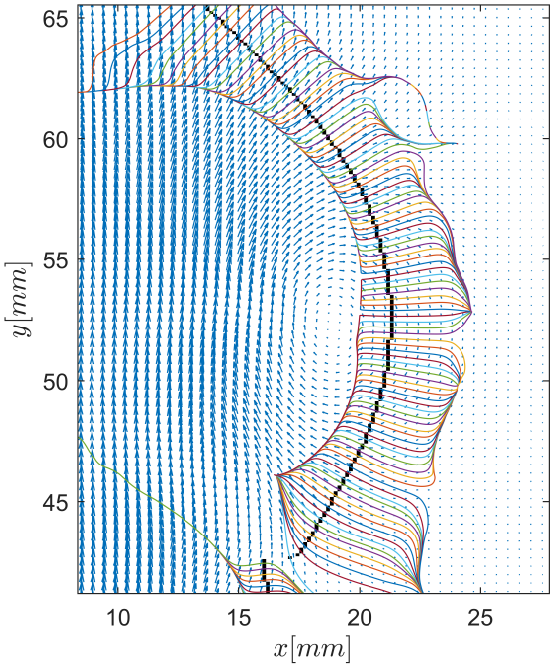

Figure 11. Velocity vectors and gradient lines for one-shot image.

In Figure 12, the vorticity profiles at 1D and 2D are shown. In Figure 12(a), the vorticity peak at 1D along gradient lines is observed to be closer to the interface than that of the peak observed using the normal sampling method, being closer to the peak observed using radial method. Moreover, the vorticity peak at 1D along gradient lines is 20% lower than that of radial lines. When going upstream these differences intensify considerably being the peak for gradient lines almost 60% lower than that of normal lines and 50% lower than that of radial lines.

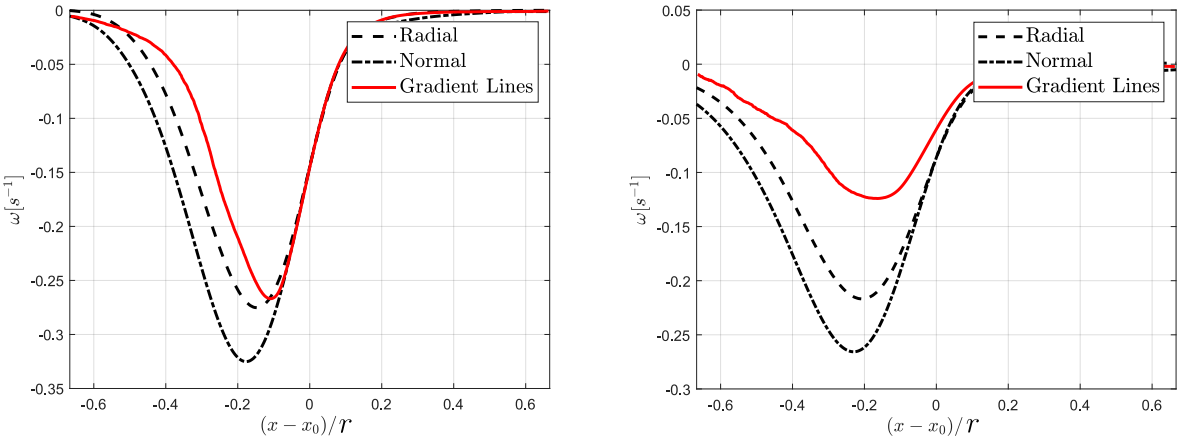

(a) 1D (b) 2D

Figure 12. Vorticity profiles at 1D and 2D using conditional statistics along the gradient lines compared to statistics in the radial and normal direction.

The turbulent kinetic energy (TKE) profiles at 1 and 2D are depicted in Figure 13. Unlike vorticity profiles, at 1D, turbulent kinetic energy along gradient lines is 15% higher than that of radial and normal profiles. Moreover, turbulent kinetic energy along gradient lines is more broadly distributed along the line but still follows the same trend as his radial and normal counterparts. In contrast, at 2D, TKE profile along gradient lines shows has a small increase when going further into the jet center from the interface. Also as opposed to the profile at 1D, the TKE values in the coflow side are increased.

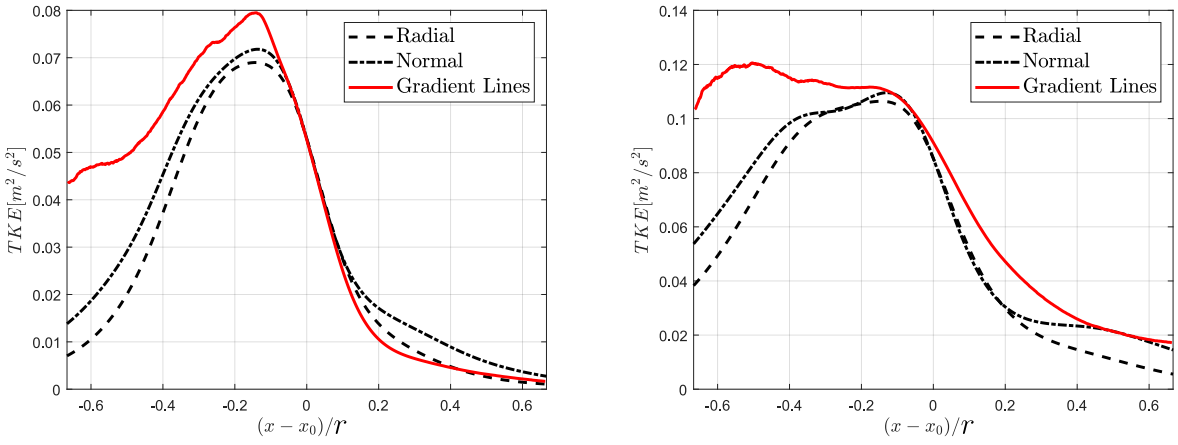

(a) 1D (b) 2D

Figure 13. Turbulent kinetic energy profiles at 1D and 2D using conditional statistics along the gradient lines compared to statistics in the radial and normal direction.

6. Conclusions

A method to obtain gradient trajectory statistics at the turbulent/Non-Turbulent interface of a jet flow has been developed. Data are compared to statistics conditioned at the TNTI using radial and normal sampling methods. According to Patiño et al. (2023), it is expected that the conditional statistics will not converge to the same results. The investigation revealed that sampling direction has a significant impact on the measured flow properties in the vicinity of the TNTI. Scalar concentration profiles indicate that eddies have a diminished effect on profiles when using gradient lines. The scalar dissipation rate is found to show a clear Gaussian distribution. Velocity magnitude and vorticity profiles show marked differences depending on the sampling direction, with gradient lines producing lower magnitudes in certain regions. The turbulent kinetic energy (TKE) was found to be higher and more broadly distributed along the gradient trajectory. These findings highlight the importance of considering the sampling direction when computing and analyzing conditional statistics in turbulent jet flows.

Acknowledgements

This work was co-funded by the European Union (ERDF) and the Région Normandie through the RIN Tremplin HYBRID project.

References

Antonia, R. A., & Zhao, Q. (2001). Effects of initial conditions on a circular jet. *Experiments in Fluids*, *31*, 319-323.

Bell, J. H., & Mehta, R. D. (1988). Contraction design for small low-speed wind tunnel. *JIAA TR*, *84*, 1-37.

Da Silva, C., Hunt, J., Eames, I., & Westerweel, J. (2014). Interfacial layers between regions of different turbulence intensity. *Annual Review of Fluid Mechanics*, *46*, 567-590.

Gampert, M., Boschung, J., Hennig, F., Gauding, M., & Peters, N. (2014). The vorticity versus the scalar criterion for the detection of the turbulent/non-turbulent interface. *Journal of Fluids Mechanics*, *750*, 578-596.

Mellado, J. P., WANG, L., & PETERS, N. (2009). Gradient trajectory analysis of a scalar field with external intermittency. *Journal of Fluid Mechanics*, *626*, 333–365. doi: 10.1017/S0022112009005886

Pasquier, N., lecordier, B., & Cessou, A. (2007). Investigation of flame propagation through a stratified mixture by simultaneous piv/lif measurements. In *Proceedings of the combustion institue.*

Patiño, F., Voivenel, L., Gauding, M., Thiesset, F., Danaila, L., & Varea, E. (2023). Influence of threshold selection on conditional statistics at the tnti of variable viscosity jets. *Proceedings of the 15th International Symposium on Particle Image Velocimetry*, *626*. doi: http://hdl.handle.net/20.500.12680/ks65hk580

Prasad, R., & Sreenivasan, K. (1989). Scalar iinterface in digital iimage of turbulent flows. *Experiments in Fluids*, *7*, 259-264.

Voivenel, L. (2016). *Influence of the hydrodynamic parameters on turbulment mixing of heterogeneous fluids. analytical and experimental study* (Unpublished doctoral dissertation). Normandie Université, Insa de Rouen.

Voivenel, L., Varea, E., Danaila, L., Renou, B., Godard, G., Vandel, A., ... Cazalens, M. (2016). Entrainment quantification in variable viscosity jets. In *18th international symposium on the application of laser and imaging techniques to fluid mechanics, lisbon, portugal.*

Wang, L. (2009a). Scaling of the two-point velocity difference along scalar gradient trajectories in fluid turbulence. *Physical Review E*, *79*(4), 046325.

Wang, L. (2009b, Apr). Scaling of the two-point velocity difference along scalar gradient trajectories in fluid turbulence. *Phys. Rev. E*, *79*, 046325. Retrieved from `https://link.aps.org/doi/10.1103/PhysRevE.79.046325` doi: 10.1103/PhysRevE.79.046325

Wang, L., & PETERS, N. (2008). Length-scale distribution functions and conditional means for various fields in turbulence. *Journal of Fluid Mechanics*, *608*, 113–138. doi: 10.1017/S0022112008002139

Westerweel, J., Fukushima, C., Pedersen, J. M., & Hunt, J. C. R. (2009). Momentum and scalar transport at the turbulent/non-turbulent interface of a jet. *Journal of luids Mechanics*, *631*, 199-230.

Westerweel, T., J.and Hofmann, Fukushima, C., & Hunt, J. C. R. (2002). The turbulent/non-turbulent interface at the outer boundary of a self-similar turbulent jet. *Experiments in Fluids*, *33*, 873-878.